Joint Frequency-Domain Adaptive Equalization and Interference Cancellation for Multi–User Space-Time Block-Coded Systems*

Waleed M. Younis, Ali H. Sayed
University of California
Los Angeles, CA 90095
{waleed,sayed}@ee.ucla.edu

Naofal Al-Dhahir
AT &T Shannon Laboratory
Florham Park, NJ 07932
naofal@research.att.com

ABSTRACT

We develop an efficient adaptive receiver for joint equalization and interference cancellation for multi–user space–time block–coded transmissions. The receiver exploits the rich code structure and allows multiple user transmissions over frequency–selective fading channels with reduced complexity and lower system overhead. The adaptation scheme is based on a recursive least–squares implementation for faster convergence; nevertheless, it exploits the code structure to attain RLS performance at LMS complexity.

1. INTRODUCTION

Increasing system capacity without requiring additional bandwidth is of major significance for spectrally–efficient high–rate wireless communication systems. Space–time block–codes (STBC) help increase reliability over wireless networks [1] and they can achieve full diversity gains with simple linear processing at the receiver. It was shown in [2] that K co–channel users, each equipped with N antennas, and transmitting uncorrelated signals can be detected with N–order diversity gains, if the receiver is equipped with $N(K-1)+1$ antennas.

However, the structure of STBC can be exploited to reduce the number of receive antennas. It was shown in [3] that only K receive antennas are needed to provide N–order diversity gains and suppress $K-1$ co–channel space–time users. A simple interference cancellation scheme for two co–channel users employing the Alamouti STBC scheme [4] was developed in [3]. It was shown that by using two transmit antennas for each user and two receive antennas at the base station, it is possible to double the system capacity by applying only linear processing at the receiver.

When implemented over frequency–selective channels, the Alamouti scheme should be implemented at a *block* not *symbol* level and combined with an effective equalization scheme to realize additional multipath diversity gains without sacrificing full spatial diversity. A low–complexity scheme that achieves this goal is the single–carrier frequency–domain–equalized (SC FDE) STBC described in [5]. This scheme combines the advantages of the Alamouti scheme with those of SC FDE [6], namely, low complexity (due to use of the FFT) and reduced sensitivity, compared with orthogonal frequency division multiplexing (OFDM), to carrier frequency offsets and nonlinear distortion (due to reduced peak to average ratio).

Now coherent joint interference cancellation, equalization, and decoding of SC FDE–STBC transmissions usually requires channel state information (CSI) at the receiver, which can be estimated using training sequences embedded in each block. Then, the optimum equalizer/decoder settings can be computed from the estimated CSI. An alternative to this two–step channel–estimate–based approach is *adaptive* equalization/decoding that does not require explicit CSI estimation and reduces system overhead. It also provides a tracking mechanism for time–variant channels.

In this paper, we develop an efficient low–complexity adaptive SC FDE–STBC algorithm for joint interference cancellation, equalization, and decoding in a multiuser environment. The operation of the algorithm is described for both training and tracking modes and it is shown to possess recursive least–squares algorithm (RLS) performance at least mean squares algorithm (LMS) complexity. This work is an extension of [7] to the multiuser case and is an adaptive implementation of the schemes in [3] and [8].

The paper is organized as follows. In Section 2, we describe the structure of STBC and review schemes for non–adaptive SC FDE–STBC and joint interference cancellation and equalization techniques with two co–channel users. The adaptive version of the SC FDE is developed in Section 3 for both training and tracking modes. Simulation results for the EDGE environment are presented in Section 4 and the paper is concluded in Section 5.

2. STBC FOR BROADBAND CHANNELS

For STBCs to achieve multi–path and spatial diversity gains on frequency–selective channels, the Alamouti scheme should be implemented at a *block not symbol* level. Several schemes have been proposed for this purpose [9]. In this section we explain the structure and equalization of the SC FDE–STBC.

2.1. The Single–User Case

We consider first the scheme where a single user equipped with two antennas is transmitting data over a wireless channel and the receiver has a single antenna. Data is transmitted from the antennas according to the following space–time coding technique [5]. Denote the n^{th} symbol of the k^{th} transmitted block from antenna i by $\mathbf{x}_i^{(k)}(n)$. At times $k=0,2,4,\cdots$, pairs of length–N blocks $\mathbf{x}_1^{(k)}(n)$ and $\mathbf{x}_2^{(k)}(n)$ (for $0 \le n \le N-1$) are generated by an information source according to the rule:

$$\mathbf{x}_1^{(k+1)}(n) = -\mathbf{x}_2^{*(k)}((-n)_N),\ \mathbf{x}_2^{(k+1)}(n) = \mathbf{x}_1^{*(k)}((-n)_N) \quad (1)$$

where $\mathbf{x}$ has a covariance matrix equal to $\sigma_x^2\mathbf{I}_N$ and $(\cdot)^*$ and $(\cdot)_N$ denote complex conjugation and modulo–N operations, respectively. In addition, a cyclic prefix is added to each transmitted block to eliminate inter–user interference (IBI) and make all channel matrices *circulant*. Also, the transmitted power from each antenna is half its value in the single–transmit case so that the total transmitted power is fixed. With two transmit and one receive antenna, the received blocks k and $k+1$ are described by

$$\mathbf{y}^{(j)} = \mathbf{H}_1^{(j)}\mathbf{x}_1^{(j)} + \mathbf{H}_2^{(j)}\mathbf{x}_2^{(j)} + \mathbf{n}^{(j)} \quad \text{for } j = k, k+1 \quad (2)$$

where $\mathbf{n}^{(j)}$ is the noise vector with a covariance matrix equal to $\sigma_n^2\mathbf{I}_N$, and $\mathbf{H}_1^{(j)}$ and $\mathbf{H}_2^{(j)}$ are the *circulant* channel matrices from the first and second transmit antennas, respectively, over block j, to the receive antenna. Applying the DFT matrix $\mathbf{Q}$ to $\mathbf{y}^{(j)}$, we get (for $j=k,k+1$)

$$\mathbf{Y}^{(j)} \triangleq \mathbf{Q}\mathbf{y}^{(j)} = \mathbf{\Lambda}_1^{(j)}\mathbf{X}_1^{(j)} + \mathbf{\Lambda}_2^{(j)}\mathbf{X}_2^{(j)} + \mathbf{N}^{(j)} \quad (3)$$

where $\mathbf{X}_i^{(j)} \triangleq \mathbf{Q}\mathbf{x}_i^{(j)}$, and $\mathbf{N}^{(j)} \triangleq \mathbf{Q}\mathbf{n}^{(j)}$, and $\mathbf{\Lambda}_1^{(j)}$ and $\mathbf{\Lambda}_2^{(j)}$ are diagonal matrices given by $\mathbf{\Lambda}_i^{(j)} \triangleq \mathbf{Q}\mathbf{H}_i^{(j)}\mathbf{Q}^*$. Using the encoding rule

*This work was partially supported by NSF grants ECS-9820765 and CCR-0208573, and by a gift from AT&T Shannon Laboratory.

(1) and properties of the DFT [10], and assuming the two channels are fixed over two consecutive blocks, we arrive at

$$\mathbf{Y} = \begin{pmatrix} \mathbf{Y}^{(k)} \\ \bar{\mathbf{Y}}^{(k+1)} \end{pmatrix} = \begin{pmatrix} \mathbf{\Lambda}_1 & \mathbf{\Lambda}_2 \\ \mathbf{\Lambda}_2^* & -\mathbf{\Lambda}_1^* \end{pmatrix} \begin{pmatrix} \mathbf{X}_1^{(k)} \\ \mathbf{X}_2^{(k)} \end{pmatrix} + \begin{pmatrix} \mathbf{N}^{(k)} \\ \bar{\mathbf{N}}^{(k+1)} \end{pmatrix} \triangleq \mathbf{\Lambda X} + \mathbf{N} \quad (4)$$

where $\bar{(\cdot)}$ denotes complex conjugation of the entries of the vector. The minimum mean square error (MMSE) estimator of $\mathbf{X}$ given $\mathbf{Y}$ is then

$$\hat{\mathbf{X}} = \left(\mathbf{\Lambda}^* \mathbf{\Lambda} + \frac{1}{SNR} \mathbf{I}_{2N} \right)^{-1} \mathbf{\Lambda}^* \mathbf{Y} \triangleq \tilde{\mathbf{\Lambda}} \mathbf{\Lambda}^* \mathbf{Y} \quad (5)$$

where $\tilde{\mathbf{\Lambda}}$ is diagonal and SNR is the signal to noise ratio at the receiver, $SNR = \sigma_x^2/\sigma_n^2$. The SC MMSE–FDE output is transformed back to time–domain where decisions are made.

2.2. The Two–User Case

By using a second receive antenna, we can double the number of users. The system block diagram is shown in Figure 1.With two receive antennas and two users (each equipped with 2 antennas), Eq. (4) generalizes to

$$\left(\begin{array}{c} \mathbf{Y}_1^{(k)} \\ \bar{\mathbf{Y}}_1^{(k+1)} \\ \hline \mathbf{Y}_2^{(k)} \\ \bar{\mathbf{Y}}_2^{(k+1)} \end{array} \right) = \left(\begin{array}{cc|cc} \mathbf{\Lambda}_{x_1} & \mathbf{\Lambda}_{x_2} & \mathbf{\Gamma}_{s_1} & \mathbf{\Gamma}_{s_2} \\ \mathbf{\Lambda}_{x_2}^* & -\mathbf{\Lambda}_{x_1}^* & \mathbf{\Gamma}_{s_2}^* & -\mathbf{\Gamma}_{s_1}^* \\ \hline \mathbf{\Gamma}_{x_1} & \mathbf{\Gamma}_{x_2} & \mathbf{\Lambda}_{s_1} & \mathbf{\Lambda}_{s_2} \\ \mathbf{\Gamma}_{x_2}^* & -\mathbf{\Gamma}_{x_1}^* & \mathbf{\Lambda}_{s_2}^* & -\mathbf{\Lambda}_{s_1}^* \end{array} \right) \left(\begin{array}{c} \mathbf{X}_1^{(k)} \\ \mathbf{X}_2^{(k)} \\ \hline \mathbf{S}_1^{(k)} \\ \mathbf{S}_2^{(k)} \end{array} \right) + \left(\begin{array}{c} \mathbf{N}_1^{(k)} \\ \bar{\mathbf{N}}_1^{(k+1)} \\ \hline \mathbf{N}_2^{(k)} \\ \bar{\mathbf{N}}_2^{(k+1)} \end{array} \right) \quad (6)$$

where $\mathbf{Y}_2^{(k)}$ and $\bar{\mathbf{Y}}_2^{(k+1)}$ are the received signals at the second receive antenna at blocks k and $k+1$, respectively, and $\mathbf{S}_1^{(k)}$ and $\mathbf{S}_2^{(k)}$ are the k^{th} transmitted blocks from the first and second antennas of the second user, respectively. In more compact form, Eq.(6) can be written as

$$\begin{pmatrix} \mathbf{Y}_1 \\ \mathbf{Y}_2 \end{pmatrix} = \begin{pmatrix} \mathbf{\Lambda}_x & \mathbf{\Gamma}_s \\ \mathbf{\Gamma}_x & \mathbf{\Lambda}_s \end{pmatrix} \begin{pmatrix} \mathbf{X} \\ \mathbf{S} \end{pmatrix} + \begin{pmatrix} \mathbf{N}_1 \\ \mathbf{N}_2 \end{pmatrix} \quad (7)$$

where $\mathbf{Y}_1$ and $\mathbf{Y}_2$ are the processed signals from the first and second antennas while $\mathbf{N}_1$ and $\mathbf{N}_2$ are the corresponding noise vectors. Moreover, $\mathbf{S}$ consists of the two subvectors representing the size-N FFTs of the information blocks transmitted from the interfering user's first and second antennas at time k. The two users can be decoupled by applying the following linear zero-forcing interference canceller:

$$\begin{aligned} \begin{pmatrix} \mathbf{Z}_1 \\ \mathbf{Z}_2 \end{pmatrix} &\triangleq \begin{pmatrix} \mathbf{I}_{2N} & -\mathbf{\Gamma}_s \mathbf{\Lambda}_s^{-1} \\ -\mathbf{\Gamma}_x \mathbf{\Lambda}_x^{-1} & \mathbf{I}_{2N} \end{pmatrix} \begin{pmatrix} \mathbf{Y}_1 \\ \mathbf{Y}_2 \end{pmatrix} \\ &= \begin{pmatrix} \mathbf{\Sigma} & \mathbf{0} \\ \mathbf{0} & \mathbf{\Delta} \end{pmatrix} \begin{pmatrix} \mathbf{X} \\ \mathbf{S} \end{pmatrix} + \begin{pmatrix} \tilde{\mathbf{N}}_1 \\ \tilde{\mathbf{N}}_2 \end{pmatrix} \end{aligned} \quad (8)$$

where $\mathbf{\Sigma} = \mathbf{\Lambda}_x - \mathbf{\Gamma}_s \mathbf{\Lambda}_s^{-1} \mathbf{\Gamma}_x$ and $\mathbf{\Delta} = \mathbf{\Lambda}_s - \mathbf{\Gamma}_x \mathbf{\Lambda}_x^{-1} \mathbf{\Gamma}_s$. It can be verified that both $\mathbf{\Sigma}$ and $\mathbf{\Delta}$ have the same orthogonal structure as $\mathbf{\Lambda}$ given by (4). Once the two users have been decoupled, the equalization procedure described by (5) can be used for each user $\{\mathbf{Z}_1, \mathbf{Z}_2\}$ to recover the original data $\{\mathbf{X}, \mathbf{S}\}$.

3. ADAPTIVE SCHEME

The joint interference cancellation and equalization technique described above requires the channels to be known at the receiver. Channel estimation is done by adding a training sequence to each block and using it to estimate the channel, which increases the system overhead. Reduction of the system overhead requires using longer blocks, which is not viable for wireless channels with fast variations. In this section, we develop an adaptive technique for joint interference cancellation and equalization of the FDE–STBC. The proposed adaptive receiver eliminates the need for adding a training sequence to each data block by using a few training blocks during initialization, then it tracks the channel variations in a decision–directed mode. In this way, the system overhead can be reduced.

Starting with Eq.(8), since $\mathbf{\Lambda}_x$ and $\mathbf{\Lambda}_s$ have the same orthogonal structure as $\mathbf{\Lambda}$ in (4), we can easily verify that both $-\mathbf{\Gamma}_s \mathbf{\Lambda}_s^{-1}$ and $-\mathbf{\Gamma}_x \mathbf{\Lambda}_x^{-1}$

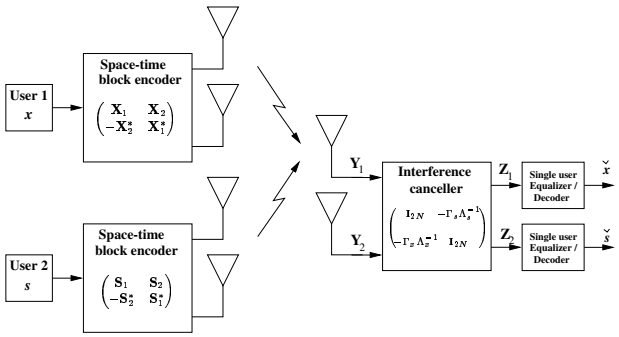

Fig. 1. Two-user system.

also have the same structure as $\mathbf{\Lambda}$ in (4). Combining the interference canceller and the MMSE equalizer, the equalizer output can be seen to be

$$\begin{aligned} \begin{pmatrix} \hat{\mathbf{X}} \\ \hat{\mathbf{S}} \end{pmatrix} &= \begin{pmatrix} \tilde{\mathbf{\Sigma}} \mathbf{\Sigma}^* & -\tilde{\mathbf{\Sigma}} \mathbf{\Sigma}^* \mathbf{\Gamma}_x \mathbf{\Gamma}_s^{-1} \\ -\tilde{\mathbf{\Delta}} \mathbf{\Delta}^* \mathbf{\Lambda}_s \mathbf{\Lambda}_x^{-1} & \tilde{\mathbf{\Delta}} \mathbf{\Delta}^* \end{pmatrix} \begin{pmatrix} \mathbf{Y}_1 \\ \mathbf{Y}_2 \end{pmatrix} \\ &\triangleq \begin{pmatrix} \mathbf{A}^1 & \mathbf{A}^2 \\ \mathbf{A}^3 & \mathbf{A}^4 \end{pmatrix} \begin{pmatrix} \mathbf{Y}_1 \\ \mathbf{Y}_2 \end{pmatrix} \end{aligned} \quad (9)$$

where

$$\tilde{\mathbf{\Sigma}} = \left(\mathbf{\Sigma}^* \mathbf{\Sigma} + \frac{1}{SNR} \mathbf{I}_{2N} \right)^{-1}, \ \tilde{\mathbf{\Delta}} = \left(\mathbf{\Delta}^* \mathbf{\Delta} + \frac{1}{SNR} \mathbf{I}_{2N} \right)^{-1}$$

and each $\mathbf{A}^i, i = 1 \cdots 4$, has the following structure

$$\mathbf{A}^i = \begin{pmatrix} \mathbf{A}_1^i & \mathbf{A}_2^i \\ \mathbf{A}_2^{i^*} & -\mathbf{A}_1^{i^*} \end{pmatrix} \quad (10)$$

Equation (9) can be written alternatively as

$$\begin{pmatrix} \hat{\mathbf{X}}_1^{(k)} \\ \hat{\mathbf{X}}_2^{(k)} \end{pmatrix} = \mathbf{U}_k^1 \begin{pmatrix} \mathbf{W}_1^1 \\ \mathbf{W}_2^1 \end{pmatrix} + \mathbf{U}_k^2 \begin{pmatrix} \mathbf{W}_1^2 \\ \mathbf{W}_2^2 \end{pmatrix} \triangleq \begin{pmatrix} \mathbf{U}_k^1 & \mathbf{U}_k^2 \end{pmatrix} \begin{pmatrix} \mathcal{W}^3 \\ \mathcal{W}^4 \end{pmatrix} \quad (11)$$

and

$$\begin{pmatrix} \hat{\mathbf{S}}_1^{(k)} \\ \hat{\mathbf{S}}_2^{(k)} \end{pmatrix} = \mathbf{U}_k^1 \begin{pmatrix} \mathbf{W}_1^3 \\ \mathbf{W}_2^3 \end{pmatrix} + \mathbf{U}_k^2 \begin{pmatrix} \mathbf{W}_1^4 \\ \mathbf{W}_2^4 \end{pmatrix} \triangleq \begin{pmatrix} \mathbf{U}_k^1 & \mathbf{U}_k^2 \end{pmatrix} \begin{pmatrix} \mathcal{W}^3 \\ \mathcal{W}^4 \end{pmatrix} \quad (12)$$

where

$$\mathbf{U}_k^i = \begin{pmatrix} \mathrm{diag}(\mathbf{Y}_i^{(k)}) & \mathrm{diag}(\bar{\mathbf{Y}}_i^{(k+1)}) \\ \mathrm{diag}(\mathbf{Y}_i^{(k+1)}) & -\mathrm{diag}(\bar{\mathbf{Y}}_i^{(k)}) \end{pmatrix}, \quad i = 1, 2 \quad (13)$$

and $\mathbf{W}_1^i$ and $\mathbf{W}_2^i$ are the vectors containing the diagonal elements of $\mathbf{A}_1^i$ and $\mathbf{A}_2^i$, respectively. Moreover, $\mathcal{W}^i$ is a $2N \times 1$ vector containing the elements of $\{\mathbf{W}_1^i, \mathbf{W}_2^i\}$, and $\mathbf{U}_k^i$ is an orthogonal matrix of size $2N \times 2N$ containing the received symbols at antenna i from blocks k and $k+1$. Equations (11) and (12) reveal the special structure of the interference canceller for the STBC problem. In the non-adaptive scenario, the coefficients of $\mathcal{W}^i$ are calculated from a channel estimate at every block. Equations (11) and (12) suggest that $\mathcal{W}^i$ can be computed adaptively, e.g., by using the RLS algorithm (for faster convergence). In this case, the receiver coefficients are updated every two blocks according to the recursions:

$$\begin{aligned} \begin{pmatrix} \mathcal{W}_{k+2}^1 \\ \mathcal{W}_{k+2}^2 \end{pmatrix} &= \begin{pmatrix} \mathcal{W}_k^1 \\ \mathcal{W}_k^2 \end{pmatrix} + \mathcal{P}_{k+2} \begin{pmatrix} \mathbf{U}_{k+2}^{1^*} \\ \mathbf{U}_{k+2}^{2^*} \end{pmatrix} \left[\mathbf{D}_{k+2}^1 - \begin{pmatrix} \mathbf{U}_k^1 & \mathbf{U}_k^2 \end{pmatrix} \begin{pmatrix} \mathcal{W}^1 \\ \mathcal{W}^2 \end{pmatrix} \right] \\ \begin{pmatrix} \mathcal{W}_{k+2}^3 \\ \mathcal{W}_{k+2}^4 \end{pmatrix} &= \begin{pmatrix} \mathcal{W}_k^3 \\ \mathcal{W}_k^4 \end{pmatrix} + \mathcal{P}_{k+2} \begin{pmatrix} \mathbf{U}_{k+2}^{1^*} \\ \mathbf{U}_{k+2}^{2^*} \end{pmatrix} \left[\mathbf{D}_{k+2}^2 - \begin{pmatrix} \mathbf{U}_k^1 & \mathbf{U}_k^2 \end{pmatrix} \begin{pmatrix} \mathcal{W}^3 \\ \mathcal{W}^4 \end{pmatrix} \right] \end{aligned} \quad (14)$$

where

$$\mathcal{P}_{k+2} = \lambda^{-1} [\mathcal{P}_k - \lambda^{-1} \mathcal{P}_k \begin{pmatrix} \mathbf{U}_{k+2}^{1^*} \\ \mathbf{U}_{k+2}^{2^*} \end{pmatrix} \mathbf{\Pi}(k) \begin{pmatrix} \mathbf{U}_{k+2}^1 & \mathbf{U}_{k+2}^2 \end{pmatrix} \mathcal{P}_k] \quad (15)$$

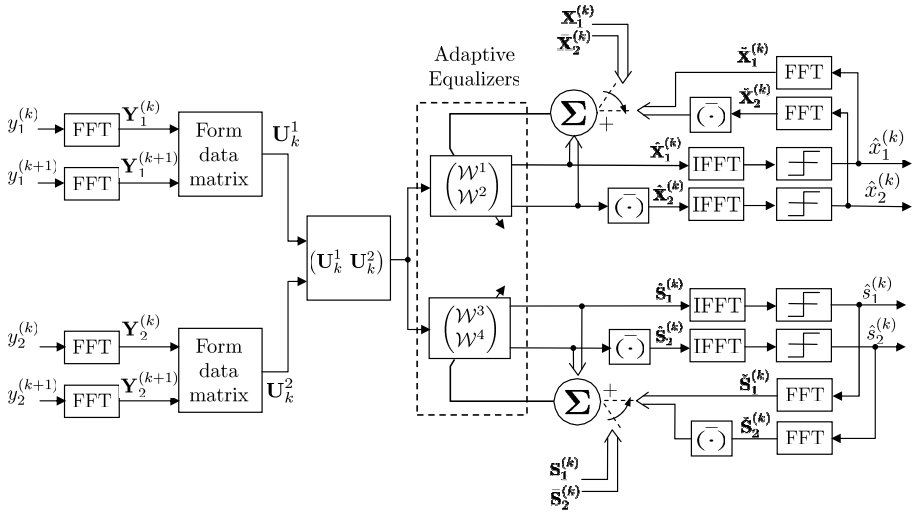

Fig. 2. Adaptive receiver structure for a 2-user system with 4-transmit 2-receive antennas.

and

$$\mathbf{\Pi}(k) = \left(\mathbf{I}_{2N} + \lambda^{-1} \left(\mathbf{U}_{k+2}^1 \;\; \mathbf{U}_{k+2}^2 \right) \mathcal{P}_k \begin{pmatrix} \mathbf{U}_{k+2}^{1^*} \\ \mathbf{U}_{k+2}^{2^*} \end{pmatrix} \right)^{-1} \tag{16}$$

and λ is a forgetting factor that is close to 1. The initial conditions are $\mathcal{W}_0^i = 0$ and $\mathcal{P}_0 = \delta \mathbf{I}_{4N}$, δ is a large number, and $\mathbf{I}_{4N}$ is the $4N \times 4N$ identity matrix. $\mathbf{D}_{k+2}^1$ and $\mathbf{D}_{k+2}^2$ are the desired response vectors given by

$$\begin{cases} \mathbf{D}_{k+2}^1 = \begin{pmatrix} \mathbf{X}_1^{(k+2)} \\ \bar{\mathbf{X}}_2^{(k+2)} \end{pmatrix} \;,\; \mathbf{D}_{k+2}^2 = \begin{pmatrix} \mathbf{S}_1^{(k+2)} \\ \bar{\mathbf{S}}_2^{(k+2)} \end{pmatrix} & \text{for training} \\ \mathbf{D}_{k+2}^1 = \begin{pmatrix} \check{\mathbf{X}}_1^{(k+2)} \\ \bar{\check{\mathbf{X}}}_2^{(k+2)} \end{pmatrix} \;,\; \mathbf{D}_{k+2}^2 = \begin{pmatrix} \check{\mathbf{S}}_1^{(k+2)} \\ \bar{\check{\mathbf{S}}}_2^{(k+2)} \end{pmatrix} & \text{for tracking} \end{cases}$$

The block diagram of the adaptive receiver is shown in Figure 2. The received signals from both antennas are transformed to the frequency domain using FFT, then the data matrices $\mathbf{U}_k^1$ and $\mathbf{U}_k^2$ in (11) and (12) are formed. $\mathbf{U}_k^1$ and $\mathbf{U}_k^2$ are passed through the filters to form the frequency domain estimates for the two users' transmitted data $\hat{\mathbf{X}}$ and $\hat{\mathbf{S}}$. These two outputs are transformed back to the time domain using IFFT and a decision device is used to generate the receiver outputs. The receiver operates in a training mode where known training data are used to generate the error vectors and update the receiver coefficients until they converge, then it switches to a decision–directed mode where previous decisions are used to update the receiver coefficients for tracking. For decision–directed operation, the reconstructed data are transformed back to frequency domain and compared to the corresponding receiver outputs to generate error vectors. The error vectors are used to update the coefficients according to the RLS algorithm. When tracking channels with fast variations, retraining blocks might be needed to prevent divergence of the algorithm.

3.1. Exploiting STBC structure

Although matrix inversion is needed in (15) for operation of the RLS algorithm, the computational complexity can be significantly reduced and matrix inversion can be avoided altogether by exploiting the special STBC structure. Actually, the complexity of the algorithm can be reduced to that of an LMS implementation! We then end up with RLS performance at LMS cost. The rationale behind complexity reduction is as follows. Starting with Eq.(15) at $k = 0$, we get

$$\mathcal{P}_2 = \lambda^{-1} [\delta \mathbf{I}_{4N} - \lambda^{-1} \delta^2 \begin{pmatrix} \mathbf{U}_2^{1^*} \\ \mathbf{U}_2^{2^*} \end{pmatrix} \cdot \mathbf{\Pi}(0) \left(\mathbf{U}_2^1 \quad \mathbf{U}_2^2 \right)] \tag{17}$$

However, $\mathbf{\Pi}(0)$ evaluates to

$$\mathbf{\Pi}(0) = \left(\mathbf{I}_{2N} + \lambda^{-1} \delta (\mathbf{U}_2^1 \mathbf{U}_2^{1^*} + \mathbf{U}_2^2 \mathbf{U}_2^{2^*}) \right)^{-1} = \begin{pmatrix} \mathbf{\Pi}_N & \mathbf{0}_N \\ \mathbf{0}_N & \mathbf{\Pi}_N \end{pmatrix} \tag{18}$$

where $\mathbf{\Pi}(0)$ is $2N \times 2N$ and $\mathbf{\Pi}_N$ is $N \times N$ diagonal and given by

$$\mathbf{\Pi}_N = (\mathbf{I}_N + \lambda^{-1} (\text{diag}(|\mathbf{Y}_1^0|^2 + |\mathbf{Y}_1^1|^2) + \text{diag}(|\mathbf{Y}_2^0|^2 + |\mathbf{Y}_2^1|^2)))^{-1}$$

Substituting (18) into (17), we find that $\mathcal{P}_2$ is given by

$$\begin{aligned} \mathcal{P}_2 &= \lambda^{-1} \delta \mathbf{I}_{4N} - (\lambda^{-1} \delta)^2 \cdot \begin{pmatrix} \mathbf{U}_2^{1^*} \mathbf{\Pi}(0) \mathbf{U}_2^1 & \mathbf{U}_2^{1^*} \mathbf{\Pi}(0) \mathbf{U}_2^2 \\ \mathbf{U}_2^{2^*} \mathbf{\Pi}(0) \mathbf{U}_2^1 & \mathbf{U}_2^{2^*} \mathbf{\Pi}(0) \mathbf{U}_2^2 \end{pmatrix} \\ &= \begin{pmatrix} \mathcal{P}_{21} & \mathcal{P}_{22} \\ \mathcal{P}_{23} & \mathcal{P}_{24} \end{pmatrix} \end{aligned} \tag{19}$$

where $\mathcal{P}_{21}$ and $\mathcal{P}_{24}$ are $2N \times 2N$ diagonal and $\mathcal{P}_{22}$ and $\mathcal{P}_{23}$ have the orthogonal structure as $\mathbf{\Lambda}$ in (4). Proceeding for $k = 2$,

$$\begin{aligned} \mathbf{\Pi}(2) &= \left(\mathbf{I}_{2N} + \lambda^{-1} \left(\mathbf{U}_4^1 \quad \mathbf{U}_4^2 \right) \mathcal{P}_2 \begin{pmatrix} \mathbf{U}_4^{1^*} \\ \mathbf{U}_4^{2^*} \end{pmatrix} \right)^{-1} \\ &= (\mathbf{I}_{2N} + \lambda^{-1} (\mathbf{U}_4^1 \mathcal{P}_{21} \mathbf{U}_4^{1^*} + \mathbf{U}_4^2 \mathcal{P}_{23} \mathbf{U}_4^{2^*} \\ &\quad + \mathbf{U}_4^1 \mathcal{P}_{22} \mathbf{U}_4^{2^*} + \mathbf{U}_4^2 \mathcal{P}_{24} \mathbf{U}_4^{2^*}))^{-1} \end{aligned} \tag{20}$$

After simple algebra, it can be verified that $\mathbf{\Pi}(2)$ has the form:

$$\mathbf{\Pi}(2) \stackrel{\triangle}{=} \begin{pmatrix} \mathbf{\Psi}_{11}(2) & \mathbf{\Psi}_{12}(2) \\ \mathbf{\Psi}_{21}(2) & \mathbf{\Psi}_{22}(2) \end{pmatrix}^{-1} = \begin{pmatrix} \mathbf{\Pi}_{11}(2) & \mathbf{\Pi}_{12}(2) \\ \mathbf{\Pi}_{21}(2) & \mathbf{\Pi}_{22}(2) \end{pmatrix} \tag{21}$$

where $\mathbf{\Psi}_{ij}(2), i, j = 1, 2$, are $N \times N$ diagonal matrices. Block matrix inversion [11] can be used to evaluate $\mathbf{\Pi}(2)$. It can be easily shown that no matrix inversion is needed since $\mathbf{\Psi}_{ij}(2), i, j = 1, 2$, are all diagonal matrices. Moreover, the $\mathbf{\Pi}_{ij}(2), i, j = 1, 2$, are $N \times N$ diagonal matrices. $\mathcal{P}_4$ is then found to be

$$\mathcal{P}_4 = \lambda^{-1} \mathcal{P}_2 - \lambda^{-1} \mathcal{P}_2 \begin{pmatrix} \mathbf{U}_2^{1^*} \\ \mathbf{U}_2^{2^*} \end{pmatrix} \mathbf{\Pi}(2) \left(\mathbf{U}_2^1 \quad \mathbf{U}_2^2 \right) \mathcal{P}_2 \tag{22}$$

It follows that $\mathcal{P}_4$ is a $4N \times 4N$ block matrix that consists of 16 $N \times N$ diagonal matrices. This means that the number of entries to be calculated is much lower than for a full matrix. If we proceed further beyond $k = 2$, we find that the structures for $\mathbf{\Pi}(k)$ and $\mathcal{P}_{k+2}$ stay the same. Table I summarizes how we can use the structure of $\mathcal{P}_{k+2}$ to update its entries. It is worth mentioning that all $N \times N$ matrices in Table I are diagonal. This means that any matrix multiplication is simply evaluated by N scalar multiplications.

4. SIMULATION RESULTS

In this section, we provide simulation results for the performance of the adaptive interference canceller and equalizer for STBC. The simulated scenario includes two co–channel users using the Alamouti STBC for frequency selective channels. Each user is equipped with two transmit antennas and 8-PSK signal constellation is used. The receiver is equipped

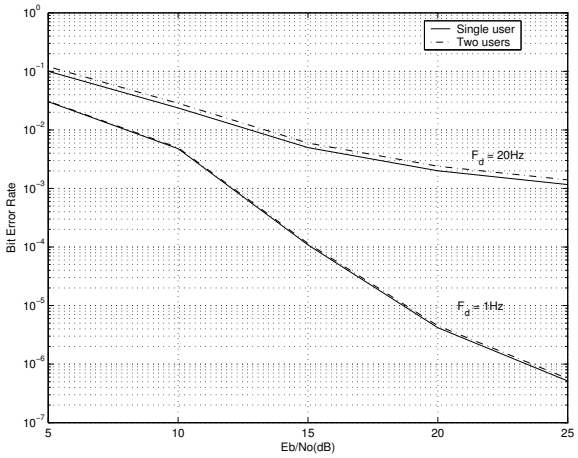

Fig. 3. BER performance of the adaptive receiver.

with 2 receive antennas. Signal to Interference Noise ratio (SINR) is set to 0dB, i.e., both users are transmitting at the same power. Data blocks of 32 symbols plus 3 symbols for the cyclic prefix are used. Typical Urban (TU) channel is considered with a linearized GMSK transmit pulse shape. Furthermore, all channels are assumed to be independent. The overall channel impulse response memory of the channel is $\nu = 3$. Figure 3 shows the bit–error–rate performance of the system compared to the single user case at two different Doppler frequencies. From this figure, it is clear that the adaptive interference cancellation technique can separate co–channel users without sacrificing performance. However, at high doppler frequencies, the RLS algorithm might not be able to track the channel variations. In this case, training more often can improve the system performance at the expense of increasing system overhead. It was shown in [7] that smaller training blocks can also be used to maintain low system overhead.

5. CONCLUSIONS

An adaptive scheme for joint interference cancellation and equalization of multi–user space–time block–coded transmission is developed. The scheme is based on a modified low–complexity RLS algorithm that exploits the rich structure of STBC to separate two equal–powered co–channel users. Both training and tracking performance results of the scheme are presented. It is shown that the system capacity can be almost doubled by using this scheme while maintaining low system complexity and overhead and without sacrificing performance or bandwidth.

6. REFERENCES

[1] A. F. Naguib, N. Seshadri, and A. R. Calderbank, "Increasing data rate over wireless channels: Space–time coding and signal processing for high data rate wireless communications," *IEEE Signal Processing Magazine*, vol. 17, no. 3, pp. 76–92, May 2000.

[2] J. H. Winters, J. Salz, and R. D. Gitlin, "The impact of antenna diversity on the capacity of wireless communication systems," *IEEE Trans. on Communications*, vol. 42, no. 2, pp. 1740–1751, February 1994.

[3] A. F. Naguib, N. Seshadri, and A. R. Calderbank, "Applications of space–time block codes and interference suppression for high capacity and high data rate wireless systems," *Proc. Asilomar Conference on Signals, Systems, and Computers*, pp. 1803–1810, Pacific Grove, CA, November 1998.

[4] S. Alamouti, "A simple transmit diversity technique for wireless communications," *IEEE Journal on Selected Areas in Communications*, vol. 16, no. 8, pp. 1451–1458, October 1998.

[5] N. Al-Dhahir, "Single-carrier frequency-domain equalization for space-time block-coded transmissions over frequency-selective fading channels," *IEEE Communication Letters*, vol. 5, no. 7, pp. 304-306, July 2001.

[6] A. Czylwik, "Comparison between adaptive OFDM and single carrier modulation with frequency domain equalization," *Proc. VTC*, pp. 865-869, May 1997.

[7] W. M. Younis, N. Al-Dhahir, and A. H. Sayed "Adaptive frequency–domain equalization of space–time block–coded transmissions," *Proc. ICASSP*, pp. 2353-2356, Orlando, FL, May 2002.

[8] A. Stamoulis, N. Al-Dhahir, A. R. Calderbank "Further results on interference cancellation and space-time block codes," *Proc. Asilomar Conference on Signals, Systems and Computers*, pp. 257-261, Pacific Grove, CA, Nov 2001.

[9] N. Al-Dhahir, M. Uysal, and C. Georghiades, "Three space-time block-coding for frequency-selective fading channels with application to EDGE," *Proc. VTC*, pp. 1834-1838, October 2001.

[10] A. Oppenheim and R. Schafer, *Discrete Time Signal Processing*, Prentice Hall, NJ, 1989.

[11] T. Kailath, *Linear Systems*, Prentice Hall, NJ, 1980.

Table I. Adaptation Algorithm

Define

$$\mathcal{P}_k \triangleq \begin{pmatrix} \mathbf{P}_{11}(k) & \mathbf{P}_{12}(k) & \mathbf{P}_{13}(k) & \mathbf{P}_{14}(k) \\ \mathbf{P}_{21}(k) & \mathbf{P}_{22}(k) & \mathbf{P}_{23}(k) & \mathbf{P}_{24}(k) \\ \mathbf{P}_{31}(k) & \mathbf{P}_{32}(k) & \mathbf{P}_{33}(k) & \mathbf{P}_{34}(k) \\ \mathbf{P}_{41}(k) & \mathbf{P}_{42}(k) & \mathbf{P}_{43}(k) & \mathbf{P}_{44}(k) \end{pmatrix}$$

where each $\mathbf{P}_{ij}(k)$ is $N \times N$ diagonal. Let

$$\mathcal{U}_k \triangleq \begin{pmatrix} \mathbf{U}_k^1 & \mathbf{U}_k^2 \end{pmatrix} = \begin{pmatrix} \mathbf{U}_{11}(k) & \mathbf{U}_{21}(k) & \mathbf{U}_{31}(k) & \mathbf{U}_{41}(k) \\ \mathbf{U}_{12}(k) & \mathbf{U}_{22}(k) & \mathbf{U}_{32}(k) & \mathbf{U}_{42}(k) \end{pmatrix}$$

where the entries of $\mathcal{U}_k$ are given by Eq. (13). Also, each $\mathbf{U}_{ij}(k)$ is $N \times N$ diagonal. $\mathcal{P}_k$ is then updated as follows:

1. Let
$$\mathbf{\Psi}_k = \mathbf{I}_{2N} + \lambda^{-1}\mathbf{U}_{k+2}\mathcal{P}_k\mathbf{U}_{k+2}^* = \begin{pmatrix} \mathbf{\Psi}_{11}(k) & \mathbf{\Psi}_{12}(k) \\ \mathbf{\Psi}_{21}(k) & \mathbf{\Psi}_{22}(k) \end{pmatrix}$$

2. Compute its block entries $\mathbf{\Psi}_{ij}(k)$, $i, j = 1, 2$, as follows:
$$\mathbf{\Psi}_{ij}(k) = \xi_{ij} + \lambda^{-1} \cdot \sum_{l=1}^{4}\sum_{m=1}^{4} \mathbf{U}_{mi}(k+2)\mathbf{P}_{ml}(k)\mathbf{U}_{lj}^*(k+2)$$
where $\xi_{ij} = \mathbf{I}_N$ when $i = j$ and $\mathbf{0}_N$ otherwise. Again, each $\mathbf{\Psi}_{ij}(k)$ is $N \times N$ diagonal.

3. Compute
$$\mathbf{\Pi}(k) = \begin{pmatrix} \mathbf{\Sigma}_\Psi^{-1}(k) & \mathbf{\Sigma}_\Psi^{-1}(k)\mathbf{\Psi}_{12}\mathbf{\Psi}_{22}^{-1} \\ \mathbf{\Psi}_{22}^{-1}\mathbf{\Psi}_{21}\mathbf{\Sigma}_\Psi^{-1}(k) & \mathbf{\Psi}_{22}^{-1}\mathbf{\Psi}_{21}\mathbf{\Sigma}_\Psi^{-1}(k)\mathbf{\Psi}_{12}\mathbf{\Psi}_{22}^{-1} \end{pmatrix}$$
where $\mathbf{\Sigma}_\Psi(k) = \mathbf{\Psi}_{11}(k) - \mathbf{\Psi}_{12}(k)\mathbf{\Psi}_{22}^{-1}(k)\mathbf{\Psi}_{21}(k)$ is the Schur complement of $\mathbf{\Psi}_{22}(k)$ and the time index (k) has been dropped for compactness. The $\mathbf{\Pi}_{ij}(k)$ blocks of $\mathbf{\Pi}(k)$ are also $N \times N$ diagonal.

4. Define $\mathbf{\Phi}_k = \mathcal{U}_{k+2}^*\mathbf{\Pi}(k)\mathcal{U}_{k+2}$. It has a structure similar to $\mathcal{P}_k$, then the $N \times N$ diagonal matrices $\mathbf{\Phi}_{ij}(k)$, $i, j = 1 \cdots 4$, are given by
$$\mathbf{\Phi}_{ij}(k) = \sum_{l=1}^{2}\sum_{m=1}^{2} \mathbf{U}_{il}^*(k+2)\mathbf{\Pi}_{lm}(k)\mathbf{U}_{jm}(k+2)$$

5. Update $\mathbf{P}_{ij}(k+2)$ as
$$\mathbf{P}_{ij}(k+2) = \lambda^{-1}\mathbf{P}_{ij}(k) - \lambda^{-1}\sum_{l=1}^{4}\sum_{m=1}^{4} \mathbf{P}_{im}(k)\mathbf{\Phi}_{ml}(k)\mathbf{P}_{lj}(k)$$

6. Repeat the previous steps for each iteration.